

WBGT ESTIMATION WITH IMAGE-BASED MEASUREMENT

Yoshihiro Yasumuro¹, Yuki Kouzuki², Hiroshige Dan³, and Taira Ozaki⁴

Abstract: Under the influence of rising temperature by the global warming and heat island by the urbanization, number of emergency patients by the heat stroke increases year after year. There are a great many cases developing the heat stroke in homes and gardens as well as streets and public facilities. The wet-bulb globe temperature (WBGT) is usually used as an index value to judge the degree of risk of the heatstroke. WBGT is a composite temperature and is derived from a formula of weighted summation of natural wet-bulb temperature, globe thermometer temperature and dry-bulb temperature. Public service only provides the WBGT information at sparse spots in a town, since WBGT is measured by spot measurement using a specific set of sensors. WBGT reflects humidity, wind speed, and visible and infrared radiation on humans as well as air temperature. The risk of the heatstroke is sometimes surprisingly close to daily life environment before you notice. This paper addresses an easy-to-handle technique to visualize the risk of heatstroke in the living environment in the users' immediate surroundings.

Keywords: Heatstroke, Wet Bulb Globe Temperature (WBGT), Structure from Motion (SFM)

1 INTRODUCTION

Due to the influence of rising temperature by the global warming and heat island by the urbanization, number of emergency patients by the heat stroke increases year after year. As shown in Fig. 1, there are a great many cases developing the heat stroke in homes and gardens as well as streets and public facilities. The wet-bulb globe temperature (WBGT) is usually used as an index value to judge the degree of risk of the heatstroke. WBGT is a composite temperature and is derived from a formula of weighted summation of natural wet-bulb temperature, globe thermometer temperature and dry-bulb temperature as expressed by equation (1). Public service only provides the WBGT information at sparse spots in a town, since WBGT is measured by spot measurement using a specific set of sensors. Especially the globe thermometer plays an important role to estimate the environmental nature of effects on heat budget for human bodies since it measures both of the explicit and implicit radiant heat of the measurement spot as the structure of the sensing unit is depicted in Figure 2. And thus the WBGT reflects humidity, wind speed, and visible and infrared radiation on humans as well as air temperature. The risk of the heatstroke is sometimes surprisingly close to daily life environment before you notice.

¹ Professor, Faculty of Environmental and Urban Engineering, Kansai University, Suita, Japan, yasumuro@kansai-u.ac.jp

² Bachelor Student, Faculty of Environmental and Urban Engineering, Kansai University, Suita, Japan

³ Associate Professor, Faculty of Environmental and Urban Engineering, Kansai University, Suita, Japan, {dan, t_ozaki}@kansai-u.ac.jp

This paper addresses an easy-to-handle technique to estimate and visualize the risk of heatstroke in the living environment in the users' immediate surroundings.

$$WBGT = 0.7 T_{\text{dry bulb}} + 0.2 T_{\text{wet bulb}} + 0.1 T_{\text{globe}} \quad (1)$$

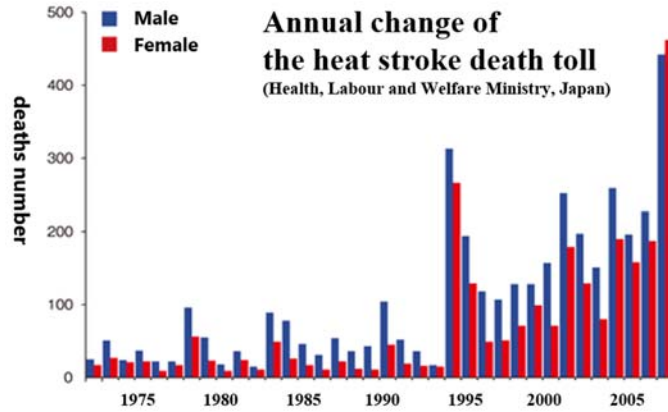


Figure 1: Annual heat stroke death toll in Japan; modified figure from web page National Institute for Environmental Studies, Japan.

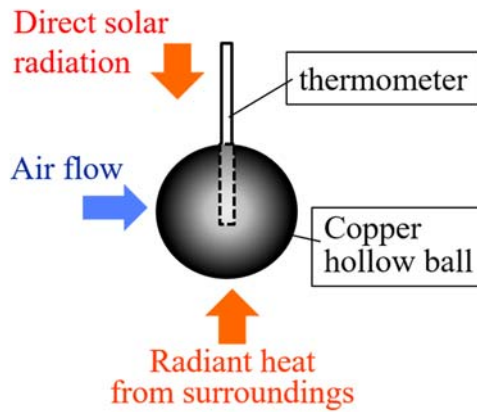


Figure 2: Schematic function of WBGT thermometer, which measures the air temperature affected by direct solar radiation, wind and surrounding radiant heat.

2 RELATED WORK

A forgoing study conducted by Ito (Ito, 2014) in Suita city at Osaka prefecture in Japan presented a good estimation of WBGT based on estimating globe thermometer temperature by multiple regression analysis instead of using actual globe thermometers. They use an equation composed by a linear combination of grade temperature, sky factor, wind factor and direct solar radiation as expressed in equation (2).

$$T_{\text{globe}} = a_1 T_S + a_2 R_S + a_3 \lambda_U + a_4 \lambda_R + c, \quad (2)$$

where a_1 - a_4 , c are the coefficients to be determined. And the other four factors are as listed below.

- T_S : ground temperature (°C)
- R_S : sky factor (%) captured by a fish-eye image
- λ_U : air flow $\begin{cases} =1 & (\text{presence}) \\ =0 & (\text{absence}) \end{cases}$
- λ_R : direct solar radiation $\begin{cases} =1 & (\text{presence}) \\ =0 & (\text{absence}) \end{cases}$

They use 47 actual measured data for multiple regression analysis to find the coefficient values and fit the equation to the measured data. This technique enables to produce WBGT distribution images covering whole blocks of the town based on aerial thermography and sky factors on ground level of the streets.

3 METHOD

3.1 Overview

While Ito used a large-scaled aerial equipment and wide-spread ground investigations for capturing WBGT distribution, we use a handy-type of thermocamera and color camera to create a WBGT image so that the individual user can visualize the potential risk pf heatstroke in the scale of user’s living environments from the first person perspective. The parameters of the grand temperature can be captured by a thermocamera and the sky factor can be estimated by 3D reconstruction technique, Structure from motion (SFM) with color photo collection of the target scene. SFM is a photogrammetry technique which provides an image-based modelling process to recover camera parameters, pose estimates, and sparse 3D scene geometry from unorganized photo collection of the scene (Snavely, 2006, Wu, 2013). We also employ a multi-view stereo technique to produce dense mesh of an entire scene (Jancosek, 2011). The produced 3D mesh model enables us to examine the sky factor by computer graphics rendering that allows to set the panoramic view to render the sky dome from the ground level, looking straight upward vertically from an arbitrary viewpoint. The other parameters of the wind factor and direct solar radiation can be 1-0 integer valuables according to the presence or absence of the wind and the direct

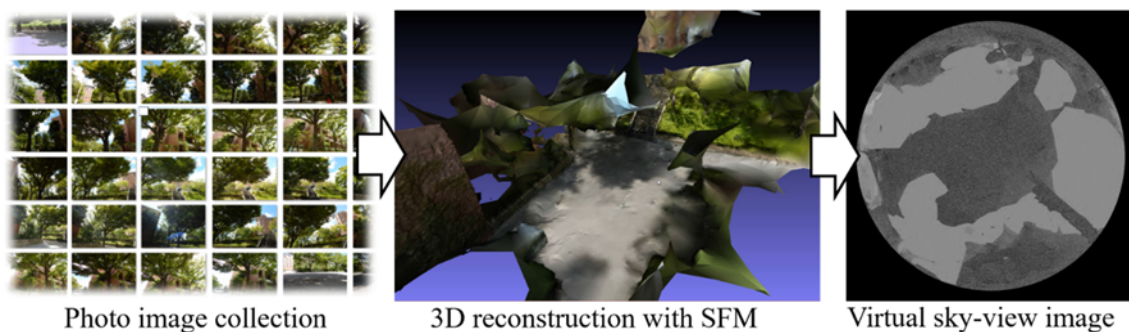


Figure 3: SFM usage for acquiring sky factor; Using a photo collection (left) of the scene, SFM reconstructs the 3D geometry (center) where upward panoramic rendering from the grand level can be used for sky-view image (right).

sunlight on the spot. Our method realizes a small-scale but easy to visualize the potential risk of the heatstroke in user’s immediate surroundings, moreover, 3D reconstruction information can be used for producing 3D version of the WBGT distribution image to understand the actual situation in front of the user.

4 EXPERIMENT

4.1 Data Collection

We conducted WBGT estimation experiment by gathering measurement data by both the proposed estimation method and actual WBGT measurement for reference at 11 places. We used a digital thermocamera (testo875, testo AG) and a digital color camera (COOLPIX L820, Nikon) to take about 50 thermography and photos of the target places. We also used a WBGT thermometer (HD32.2, Tsuruga Electric Corp.) and a wide-angle camera (Kodak PIXPRO SP360, Maspro Denkoh Corp.) to acquire the reference of the ground truth of WBGT value and the sky factor for each place. We divide the measured data sets into 4 categories, according to the combinations of the presence and the absence of wind and direct solar radiation at the measured spots. Then globe thermometer temperature equation is determined by fitting the acquired data with least squares method for each category.

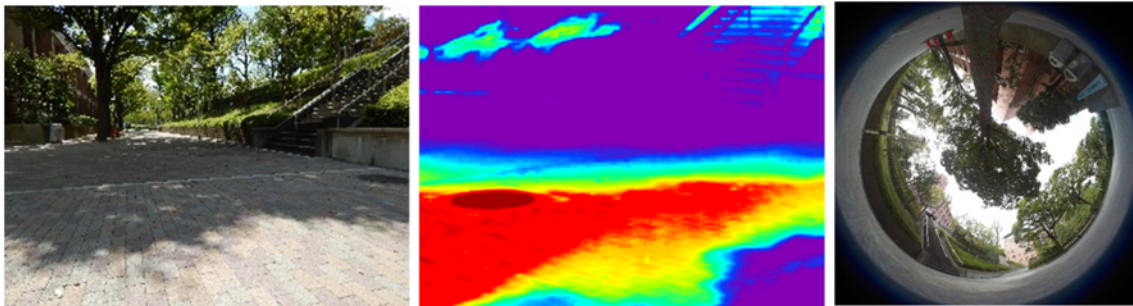


Figure 4: Example of the sampled data; color photo (left) and thermal image (center) and sky-view image reference captured by a fish-eye camera (right)

Table 1: Result of the Estimation

Solar radiation existence	N	Y	N	Y
Wind existence	N	N	Y	Y
T_{globe} avg. error (°C)	1.25	1.79	0.03	1.58
(std. dev. (°C))	0.95	1.32	0.05	0.88
WBGT avg. error (°C)	0.32	0.37	0.03	0.38
(std. dev. (°C))	0.26	0.26	0.05	0.46
# of samples	11	12	4	6

5 CONCLUSIONS

As shown in Table 1, although sky factor estimation using 3D models constructed by SFM gives 36.5 % of error in average (14.1 % in standard deviation), the equation for estimating globe thermometer temperature holds quite small weight of coefficient for the sky factor in the result of the data fitting. Then, globe thermometer temperature can be estimated with 1.3 °C error in average at the worst case among the 4 categories. Finally WBGT estimation can be precisely done within error of 0.38 °C in average and 0.46 °C in standard deviation for 11 places in total. WBGT estimation can be done for each pixel in the thermography images and WBGT distribution image can be created by converting the temperature values from thermography. This also can be mapped onto 3D models of the target scene created by SFM, so the user can visually assure the distribution of the regions of possible heatstroke risk and safe regions in the target scenery in front of the user as shown in the Figure 4. Since a smartphone can take thermal imagery with a small attachment lately, developing an all-in-one application software for a mobile device is our future work.

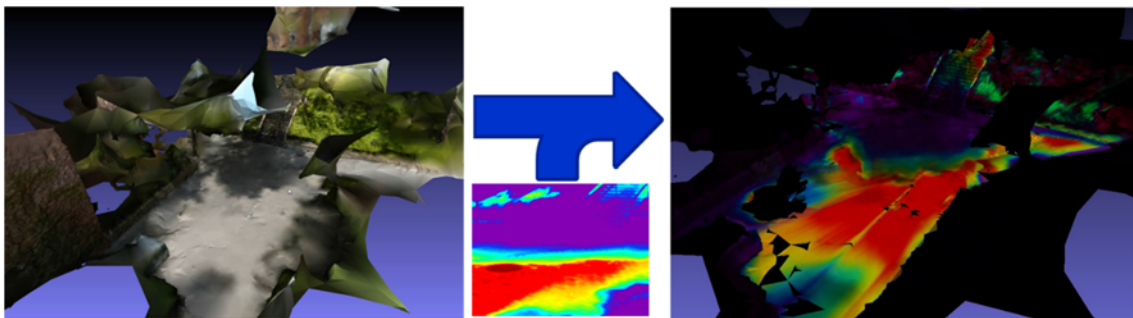


Figure 5: WBGT-mapped version of the 3D scene

ACKNOWLEDGMENTS

This research is partially supported by The Organization for Research and Development of Innovative Science and Technology (ORDIST) in Kansai University and Japan Society for the Promotion of Science (JSPS) Grants-in-Aid for Scientific Research (15H02983).

REFERENCES

- National Institute for Environmental Studies, Japan. Web page (in Japanese): <https://www.nies.go.jp/kanko/kankyogi/32/10-11.html> (checked in Jan. 2017)
- Daigo Ito, Shinichi Morita, Katsuya Tanaka, Keiji Goto, Kirio Shimizu, Akiko Misasa, Analysis of Land Surface Temperature and Hot Environment by using the Thermal Image Data, Journal of Heat Island Institute International Vol.9 (2014), pp.23-31.(in Japanese)
- Snively, N., Seitz, S. M., and Szeliski, R. D. (2006). Photo tourism: Exploring photo collections in 3D, ACM Transactions on Graphics (SIGGRAPH Proceedings), 25 (3), 835-846.
- Wu, C. (2013). Towards linear-time incremental structure from motion, International Conference on 3DTV, pp. 127-134.
- Jancosek M. et al., (2011), Multi-View Recon-struction Preserving Weakly-Supported Surfaces, CVPR 2011, pp.3121-3128.